



ESA Cryosat Plus for Oceans

Validation Report: WP5000 Global wet tropospheric correction (U. Porto)

Reference: CLS-DOS-NT-14-081
Nomenclature: CP40-WP5000-VR-01
Issue: 1. 0
Date: May. 20, 14





Chronology Issues:			
Issue:	Date:	Reason for change:	Author
1.0	20/05/14	Creation of Issue 1.0 document	M. Raynal T. Moreau

People involved in this issue:		
Written by (*):	M. Raynal (CLS) T. Moreau (CLS)	Date + Initials:(visa or ref)
Checked by (*):	S. Labroue (CLS)	Date + Initial:(visa ou ref)
Approved by (*):	J. Fernandes (U.Porto)	Date + Initial:(visa ou ref)
Application authorized by (*):	(ESA) N. Picot (CNES)	Date + Initial:(visa ou ref)

**In the opposite box: Last and First name of the person + company if different from CLS*

Index Sheet:	
Context:	
Keywords:	[Mots clés]
Hyperlink:	

Distribution:		
Company	Means of distribution	Names
CLS	Notification	



List of tables and figures

List of tables:

Aucune entrée de table d'illustration n'a été trouvée.

List of figures:

Figure 1: The mode mask, uploaded to CryoSat-2 in July 2012 (left panel) and January 2013 (right panel) (from http://cryosat.mssl.ucl.ac.uk/qa/mode.php).....	2
Figure 2: Default values for the DComb WTC in July 2012 (left panel) and January 2013 (right panel).....	2
Figure 3: Along track number of observations from the DComb WTC solution, in July 2012 (left panel) and January 2013 (right panel)	3
Figure 4: Along track formal error from the DComb WTC solution, in July 2012 (left panel) and January 2013 (right panel)	3
Figure 5: Map of the mean along track (DComb - ECMWF) difference in m (left panel), and map of the mean standard deviation of along-track (DComb - ECMWF) difference in m (right panel) averaged in (2degx2deg) geographical bins through July 2012.....	5
Figure 6: Mean along track (DComb - ECMWF) difference as function of the latitude (left panel) and the coastal distance (right panel).	5
Figure 7: Maps of the mean along track gain of variance between SLA computed with DComb and ECMWF WTCs, averaged in (2degx2deg) geographical bins through July 2012 (left panel) and January 2013 (right panel).	6
Figure 8: Maps of the mean along track gain of variance between SLA computed with DComb and ECMWF WTCs, averaged in (2degx2deg) geographical bins through July 2012 (left panel) and January 2013 (right panel), after smoothing.	6
Figure 9: Mean along track gain of variance between SLA computed by using the DComb and the ECMWF WTCs as function of the latitude (left panel) and the coastal distance (right panel) in July 2012.....	7
Figure 10: Maps of mean SSH differences at crossovers averaged in (4degx4deg) geographical bins through July 2012, for the DComb (left panel) and the ECMWF (right panel) solutions.	7
Figure 11: Maps of the mean difference of variance of SSH crossover computed with the DComb solution and with the ECMWF model, averaged in (4degx4deg) geographical bins through July 2012 (left panel) and January 2013 (right panel).	8
Figure 12: Maps of the mean difference of variance of SSH crossover computed with the DComb solution and with the ECMWF model, averaged in (4degx4deg) geographical bins through July 2012 (left panel) and January 2013 (right panel), after smoothing.	8
Figure 13: Mean difference of variance of SSH crossover difference computed with the DComb solution and with the ECMWF model, as function of the latitude for July 2012 (right panel) and January 2013 (left panel).	9
Figure 14: (Left panel) ECMWF WTC from U. Porto dataset (red), ECMWF WTC updated at CLS (green) and the DComb WTC (blue) along the track 82 cycle 32 as function of the latitude. (Right panel). The associated flags for ECMWF, GNSS and SI_MWR.	9
Figure 15: (Left panel) ECMWF WTC from U. Porto dataset (red), ECMWF WTC updated at CLS (green) and the DComb WTC (blue) along the track 82 cycle 32 as function of the latitude. (Right panel). The associated flags for ECMWF, GNSS and SI_MWR.	10
Figure 16: Map of the differences of the WTC computed with the ECMWF model from U. Porto and with the Gaussian ECMWF grid model in July 2012 (left panel) and January 2013 (right panel).....	10



Applicable documents

Reference documents

RD 1 Manuel du processus Documentation
CLS-DOC

**Acronyms List**

CLS	Collecte Localisation Satellite
CPP	Cryosat Processing Prototype
ECMWF	European Center for Medium Range Weather Forecasts
ESA	European Space Agency
GNSS	Global Navigation Satellite System
LRM	Low Resolution Mode
MWR	Microwave Radiometer
NA	Not Applicable
OA	Objective Analysis
RD	Reference Document
RDSAR	Reduced Synthetic Aperture radar
SAR	Synthetic Aperture radar
SIRAL	Synthetic Aperture Interferometric Radar Altimeter
SLA	Sea level Anomalies
SSH	Sea Surface Haight
WTC	Wet Tropospheric Correction



List of Contents

1. Introduction	1
1.1. Purpose and scope	1
1.2. Document structure	1
2. Data and method overview	2
2.1. Data coverage and period	2
2.2. Method description	3
2.2.1. DComb WTC (U. Porto)	3
2.2.2. ECMWF WTC	4
2.2.3. Edited data	4
3. Validation results and overall assessment	4
3.1. Along track differences of the WTC	4
3.2. Along track gain of variance of SLA	6
3.3. SSH crossover differences	7
3.4. Crossover gain of variance	8
3.5. Along track analysis	9
4. Conclusion	10
5. References	11



1. Introduction

1.1. Purpose and scope

This document aims at analysing the innovative DComb Wet Tropospheric Correction (WTC) developed by the University of Porto for the CryoSat-2 mission, in comparison with the WTC estimated by using the European Center for Medium Range Weather Forecasts (ECMWF) operational model grids. A set of dedicated diagnoses has been used to evaluate the quality of this correction over ocean and see if it may improve the sea-level anomaly calculation.

The description and the analysis of all the differences that are reported herein were discussed in a strong scientific collaboration with the algorithm expert/responsible who provided a very useful support to assess the performances of their model, help to identify any unexpected behaviours and finally validate the content of this report.

1.2. Document structure

This document is structured into an introductory chapter followed by three chapters describing:

- the data used and coverage, and a short description of the two geophysical correction methods (section 2),
- the analysis of the results from the different diagnoses that are used to establish their performance (quantifying their skills and drawbacks) and their difference (section 3), and
- a discussion about these results (section 4).



2. Data and method overview

2.1. Data coverage and period

Two sets of CryoSat-2 sea level anomalies (SLA) have been computed, using the DComb and the ECMWF WTCs, at the same 1-Hz point locations along the CryoSat-2 tracks that were collated in WP3000 and WP4000, for the following two periods: July 2012 and January 2013. This includes all LRM data and most of SAR mode data over ocean (except data from the instrument SARin mode regions) as shown in Figure 1.

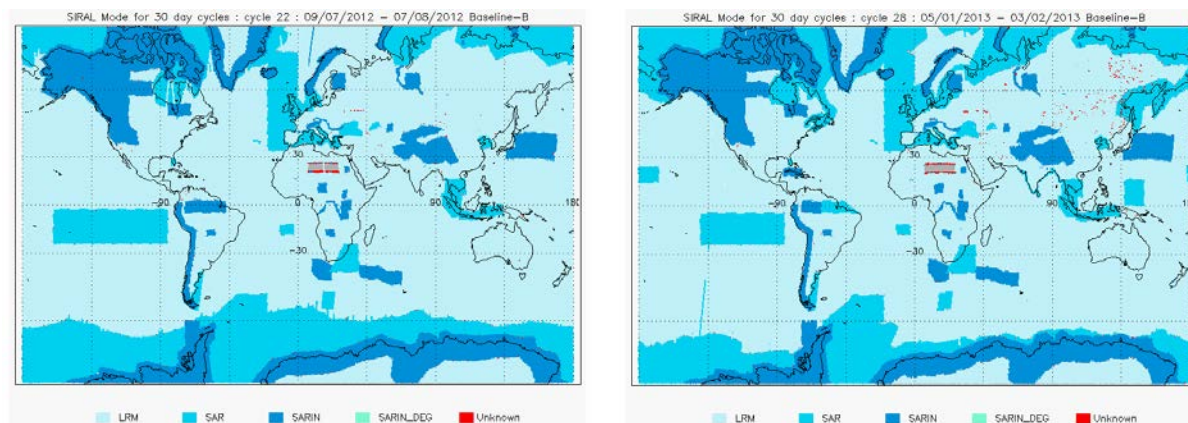


Figure 1: The mode mask, uploaded to CryoSat-2 in July 2012 (left panel) and January 2013 (right panel) (from <http://cryosat.mssl.ucl.ac.uk/qa/mode.php>).

Two sets of files containing the DComb WTC for CryoSat-2 were delivered by the U. Porto. The one which is computed for files provided by ESA is retained as the validation data for assessing the model. The Figure 2 represents the missing points within this dataset. Several tracks with default values are reported due to missing data in the ESA Level 2 GDR products and should be further investigated by ESA operational ground segment team. The missing data do not impact the WTC assessment. Also note that the default values vary in time. Indeed a higher number of default values occur in July 2012 compared to the January 2013 period.

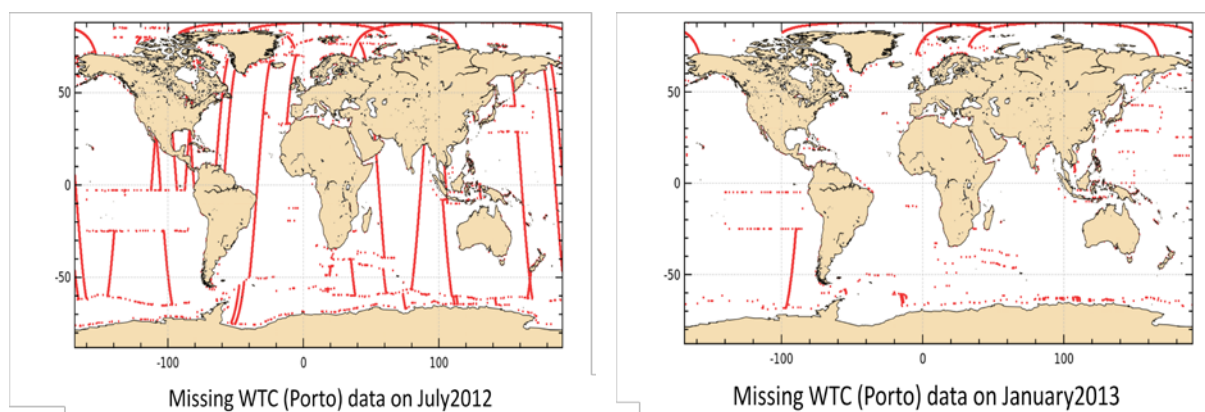


Figure 2: Default values for the DComb WTC in July 2012 (left panel) and January 2013 (right panel)

The DComb WTC dataset is time tagged differently at 1 Hz compared to the Cryosat Processing Prototype (CPP), the Dcomb WTC are thus computed by interpolation at each 1-Hz CPP point location within the CLS database. This collocation process allows more accurate comparisons.



2.2. Method description

2.2.1. DComb WTC (U. Porto)

This method combines through an objective analysis (OA) [Fernandes et al., 2010]:

- the wet path delay estimations derived from observations made by the Microwave Radiometers (MWR) on board other remote sensing satellites, and
- the wet path delay estimations from Global Navigation Satellite System (GNSS) coastal stations and from the ECMWF meteorological model.

For this study, the WTC is computed at each location and time tag along the CryoSat-2 tracks.

The quality of this correction would normally depend on the number of available sensors and the intrinsic sensor errors (and also on the formal error). The following Figure 3 shows the total number of observations used to compute the DComb WTC value at each point location. We observe high differences between July 2012 and January 2013, with a higher number of available sensors in January 2013. This should result in a better quality of the correction on the period of January.

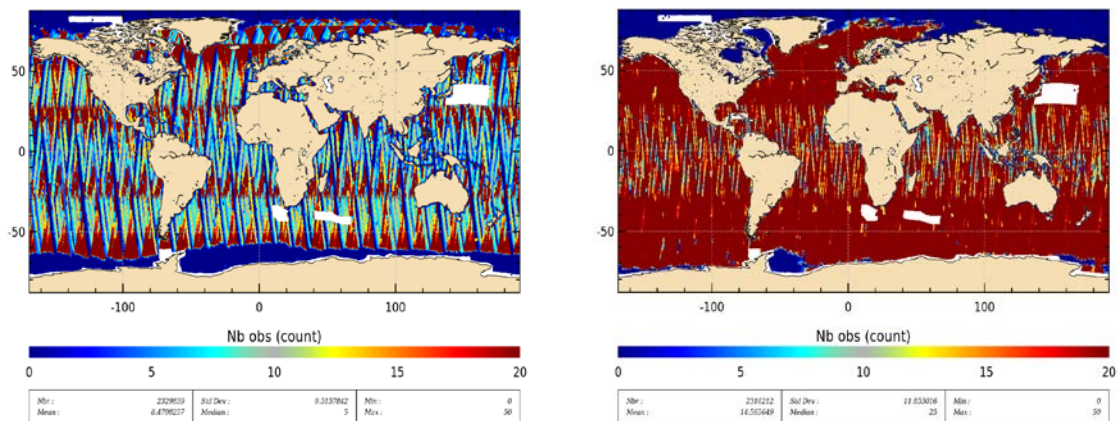


Figure 3: Along track number of observations from the DComb WTC solution, in July 2012 (left panel) and January 2013 (right panel)

We can also notice that the formal error of the DComb WTC is higher in July 2012 since the number of observations is smaller than in January 2013.

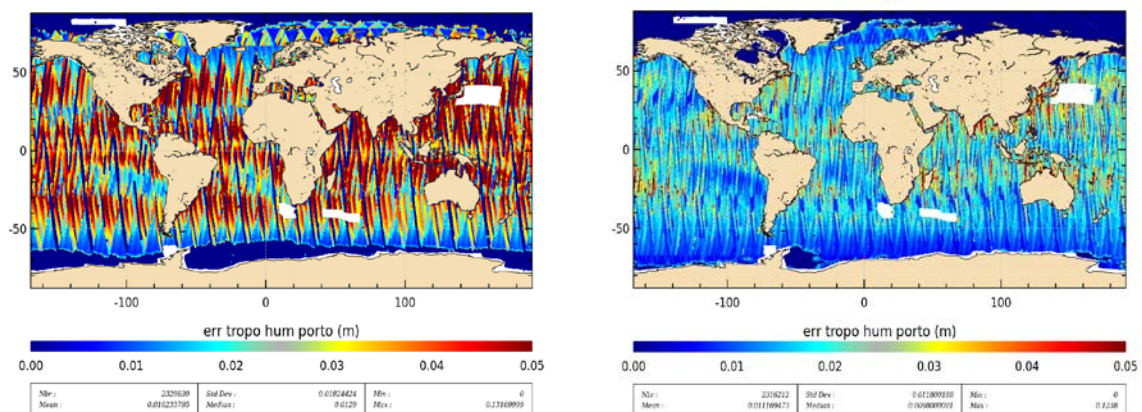


Figure 4: Along track formal error from the DComb WTC solution, in July 2012 (left panel) and January 2013 (right panel)



2.2.2. ECMWF WTC

The ECMWF models run on Gaussian global grids with an approximate resolution of 0.125° and a temporal resolution of 6 hours. The Gaussian ECMWF grids are considered for this comparison exercise since it is likely to be more accurate than the older version based on Cartesian grids.

The WTC model is computed at the altimeter time-tag from the interpolation of two meteorological fields that surround the altimeter time-tag. A WTC must be added (negative value) to the instrument final range to correct this range measurement for wet tropospheric range delays of the radar pulse.

2.2.3. Edited data

Data editing is necessary to remove altimeter measurements having lower accuracy. To analyze the consistency between both wet troposphere solutions in open ocean, only valid ocean data are selected (removing data corrupted by sea ice and rain). Specific editing criteria are applied, based on thresholds on different parameters.

3. Validation results and overall assessment

The overall objective of this validation exercise is to determine whether the DComb WTC solution allows to obtain or not a better description of the SLA as it is theoretically expected since it used measurements from MWR on board remote sensing satellites.

For this purpose, the validation of the DComb WTC is performed through the following diagnoses:

- along track comparison with ECMWF WTC to highlight differences,
- along track and crossover gain of variance of SLA to determine which correction shows the best performances.
- study of the DComb WTC transition where few MWR measurements are available to give an idea of the operational behaviour of this solution.

The assessment task is conducted with robust and standard methods that have already been used in the Sea Level CCI project.

3.1. Along track differences of the WTC

We performed along track differences between the DComb and the ECMWF WTCs. The figure 5 shows the map of the mean (left panel) and standard deviation (right panel) of the differences averaged into $2^\circ \times 2^\circ$ bins. Higher values are observed in the equatorial band (mean as high as 2 cm), and to a lesser extent at the border of the LRM-mode zones in high latitudes. This shows that the DComb WTC under estimates the wet situations (warm pool), compared to the model correction. These differences are between 0 and 1 cm for the mid-latitudes. Also note that at higher latitudes where the sensor observations are not available, the mean and standard deviation of the difference are close to zero as the DComb WTC uses exclusively ECMWF measurements.

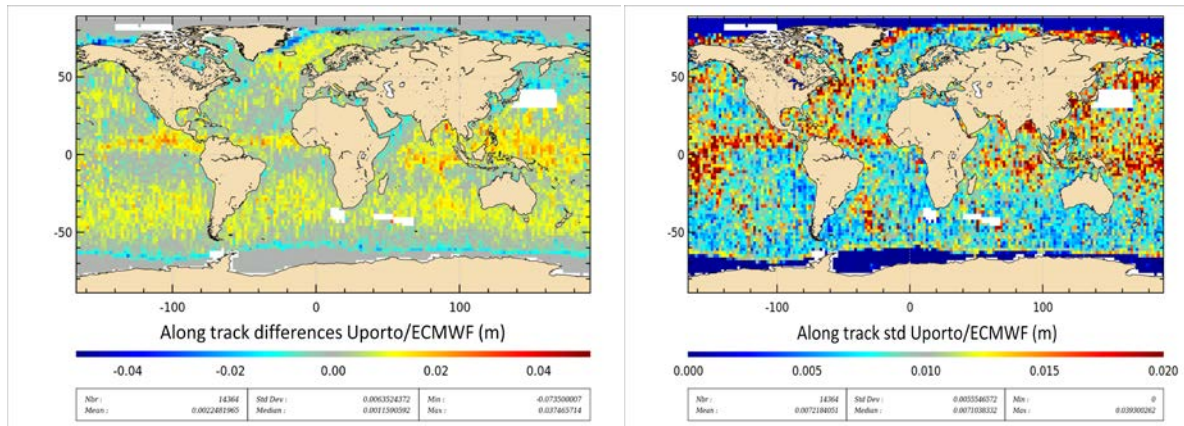


Figure 5: Map of the mean along track (DComb - ECMWF) difference in m (left panel), and map of the mean standard deviation of along-track (DComb - ECMWF) difference in m (right panel) averaged in (2degx2deg) geographical bins through July 2012.

The Figure 6 (left panel) shows that the mean (DComb - ECMWF) difference is higher in the equatorial zone and in the south hemisphere, as already observed in the preceding figure. The right panel of the Figure 6 is the mean (DComb - ECMWF) difference as function of distance from the coast. These differences are very low near coasts (<20km) where radiometer measurements become invalid due to the land contamination in the radiometer footprint. In the coastal strip, the DComb WTC is switched to the less accurate ECMWF WTC interpolated at the altimeter measurement location. For higher distance from the coast the mean difference increases.

It is difficult to analyze the DComb WTC behavior in coastal zones with statistics on a global data sets. A regional analysis focused on GNSS data used in the DComb computations would possibly allows to see locally higher differences. However the impact of the GNSS data in the WTC (occurring notably in Europe coastal zones) is not noticed on the global analysis.

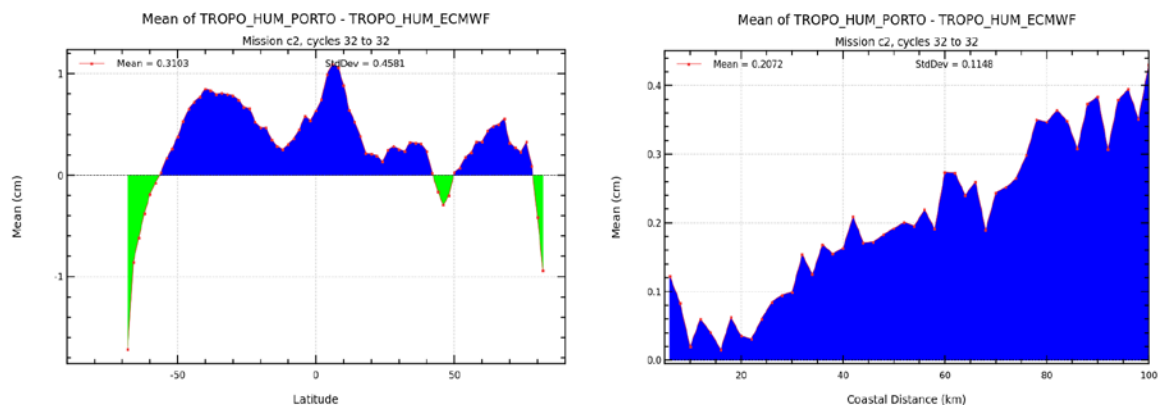


Figure 6: Mean along track (DComb - ECMWF) difference as function of the latitude (left panel) and the coastal distance (right panel).

To conclude this part, low along track differences (lower than 2cm) between the DComb WTC and the ECMWF WTC are reported which vary in latitude and coastal distance.



3.2. Along track gain of variance of SLA

After characterizing the differences between each solution, we have to determine now which one is the most accurate.

For this purpose, we computed the difference of variance between SLA with the DComb WTC and SLA with the ECMWF WTC, and check which one has the lower variance corresponding to a better data quality. These differences in variance of SLA are slightly negative (a reduction of the variance of $\sim -0.15\text{cm}^2$ which is about 0.3% of the SLA variance, meaning that this figure is not significant). The map of the geographical distribution of this difference appears to be relatively evenly distributed (see Figure 7).

By filtering out high frequency signals (with a 2D median convolution), the map of difference better highlights the difference of variance at larger length scale. The Figure 7 shows the smoothed variance difference computed in 2×2 degree geographical bins. In the equatorial band, where highest (DComb - ECMWF) differences were observed, performances are slightly better for the DComb WTC solution (considering the negative values of the variance difference). We observe also more variability of the gain of variance of SLA in January (including the south hemisphere where the humidity content is higher than for the remainder of the year). On the opposite the DComb WTC slightly degrades the performance for higher latitudes (dry atmospheres), especially in the south hemisphere.

A noticeable better reduction of SLA variance is obtained in January 2013 as expected since the number of MWR observations is higher for this month.

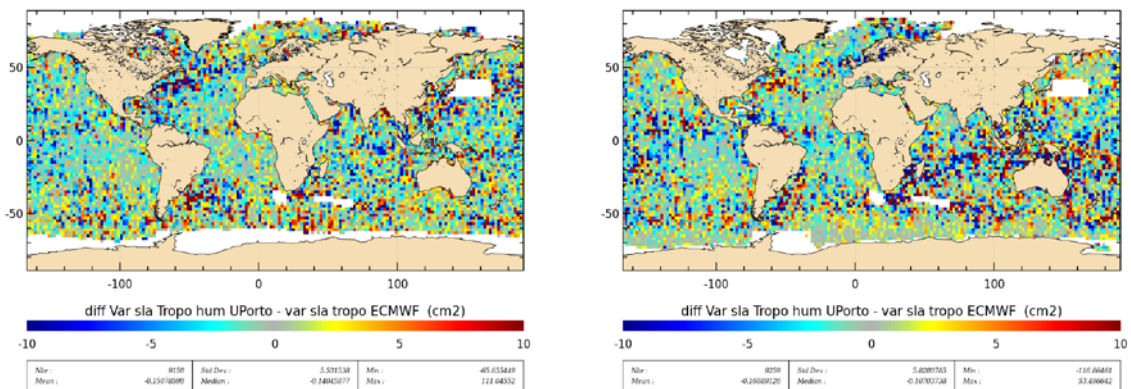


Figure 7: Maps of the mean along track gain of variance between SLA computed with DComb and ECMWF WTCs, averaged in (2degx2deg) geographical bins through July 2012 (left panel) and January 2013 (right panel).

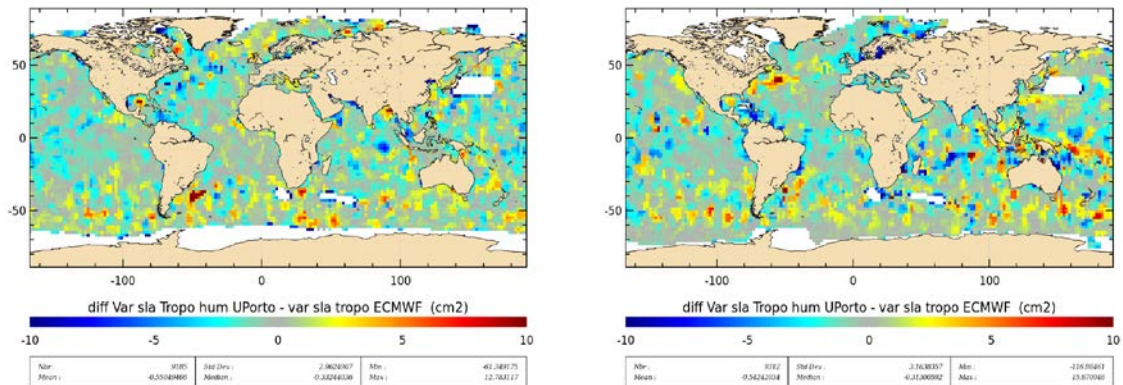


Figure 8: Maps of the mean along track gain of variance between SLA computed with DComb and ECMWF WTCs, averaged in (2degx2deg) geographical bins, after smoothing.



The reduction of variance computed globally is also obtained in both open ocean and coastal regions, and particularly for low latitudes and close to the coasts where the differences in variance are clearly negative as shown on the Figure 9 (about 2.4cm² at distance lower than 100km).

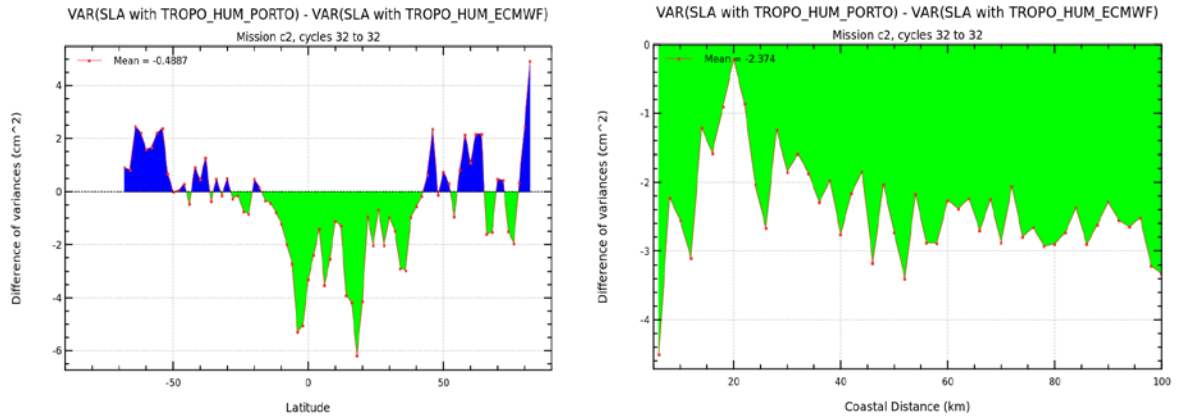


Figure 9: Mean along track gain of variance between SLA computed by using the DComb and the ECMWF WTCs as function of the latitude (left panel) and the coastal distance (right panel) in July 2012.

To conclude this part, the along-track gain of variance diagnosis shows that the DComb WTC improves the performance between 50S and 50N whereas it degrades the performance for dry atmosphere at higher latitudes.

3.3. SSH crossover differences

Analysis (mean and standard deviation) on crossovers also shows the improvement of the new solution. For this diagnosis, to perform the crossover calculation we filter out high oceanic variability (above 20cm).

Maps of mean sea surface height (SSH) differences at crossovers between ascending and descending tracks are computed with on one hand the DComb WTC (Figure 10 right) and on the other hand the ECMWF WTC (Figure 10 left). These figures show no difference on the crossover mean map.

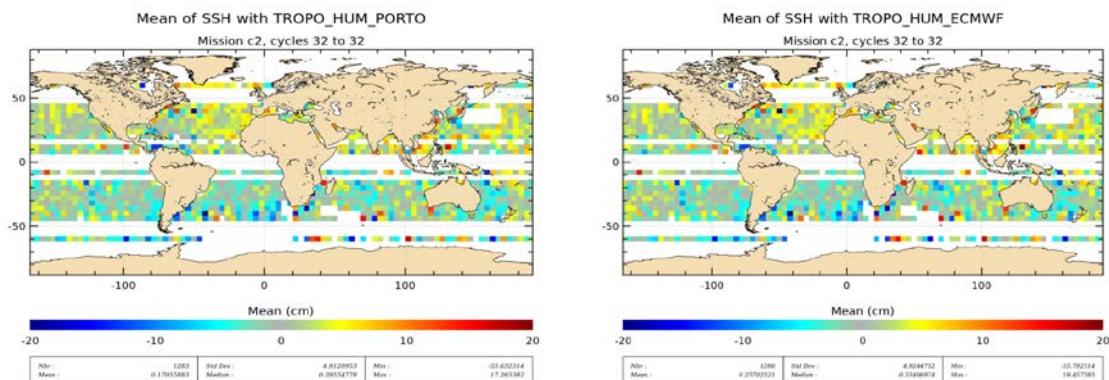


Figure 10: Maps of mean SSH differences at crossovers averaged in (4degx4deg) geographical bins through July 2012, for the DComb (left panel) and the ECMWF (right panel) solutions.



This diagnosis doesn't show improvement of SSH reduction at crossovers.

It should be emphasized that this result is based on crossover points that are located in mid-latitude bands only, due to the particular CryoSat-2 orbit which does not exhibit crossing of ascending and descending arcs in equatorial band and at high latitudes (for 10days maximum of lag time).

3.4. Crossover gain of variance

The difference in variance of SSH crossover difference is used as a good indicator for establishing the performance of the WTC solution. A global positive impact (reduction, in average, of variance by about 1.16 cm² which is 2.5% of crossover SSH differences in July 2012, and 0.6cm² or 1.4% in January 2013) of the DComb solution has been computed (see Figure 11), which confirm the preceding results obtained with along-track SLA gain of variance. This result is obtained by selecting crossovers between -50° and +50° of latitudes. The gain is degraded by considering high-latitudes crossovers when performing the global statistic as observed on along track SLA diagnosis (2.3% and 1.2% for July 2012 and January 2013 respectively).

Figure 10 shows after smoothing the global variance reduction that corroborates this tendency. Note that, due to the too small number of CryoSat-2 crossovers at low latitudes, statistics at crossovers are only determined in the mid-latitude bands for the two selected months period. Figure 11 shows in addition that this reduction is higher for low latitudes.

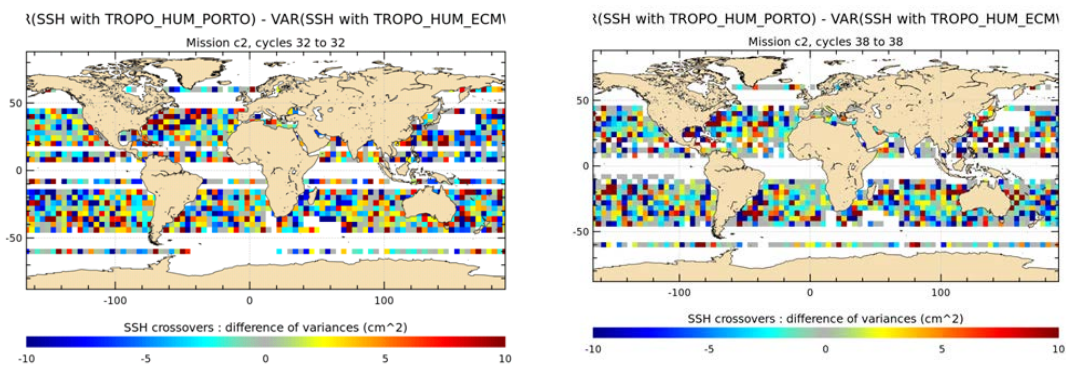


Figure 11: Maps of the mean difference of variance of SSH crossover computed with the DComb solution and with the ECMWF model, averaged in (4degx4deg) geographical bins through July 2012 (left panel) and January 2013 (right panel).

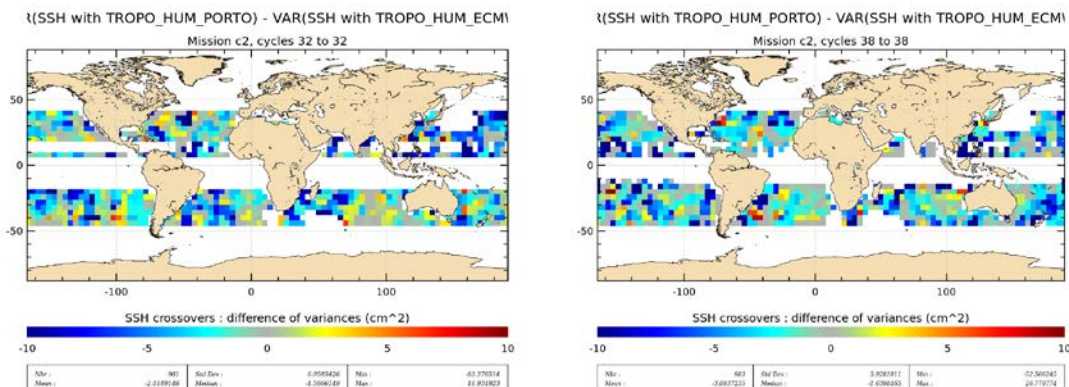


Figure 12: Maps of the mean difference of variance of SSH crossover computed with the DComb solution and with the ECMWF model, averaged in (4degx4deg) geographical bins through July 2012 (left panel) and January 2013 (right panel), after smoothing.



Figure 13 confirms that the reduction of variance is higher at low latitudes.

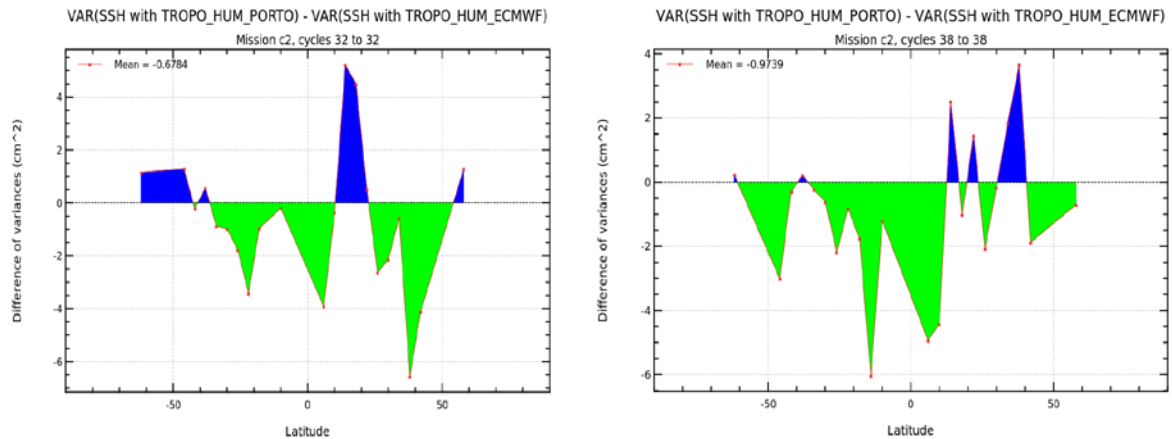


Figure 13: Mean difference of variance of SSH crossover difference computed with the DComb solution and with the ECMWF model, as function of the latitude for July 2012 (right panel) and January 2013 (left panel).

3.5. Along track analysis

In this part of the assessment we analyse the DComb WTC along track plots as shown in Figure 14 and Figure 15.

From these figures, one can notice the presence of some little discontinuities of the DComb WTC (up to few mm) that are likely to be related to changes of the ECMWF flag. When the number of observations is lower than 4, the less accurate ECMWF WTC is used in the AO processing scheme to compute the DComb WTC final value, degrading the quality of the WTC at the current point and creating a noticeable discontinuity in WTC that is not physical. As a result, it also impacts the SLA. An interpolation solution on few kilometres discontinuities could be considered. The DComb algorithm could be improved by propagating the radiometer WTC up to the change of flag but imposing the ECMWF dynamics to reduce these discontinuities.

Also note that over land or near the coasts the radiometric measurements which generally fail is superseded by a correction computed from the ECMWF meteorological model in the DComb WTC, as expected (see illustration in figure 13).

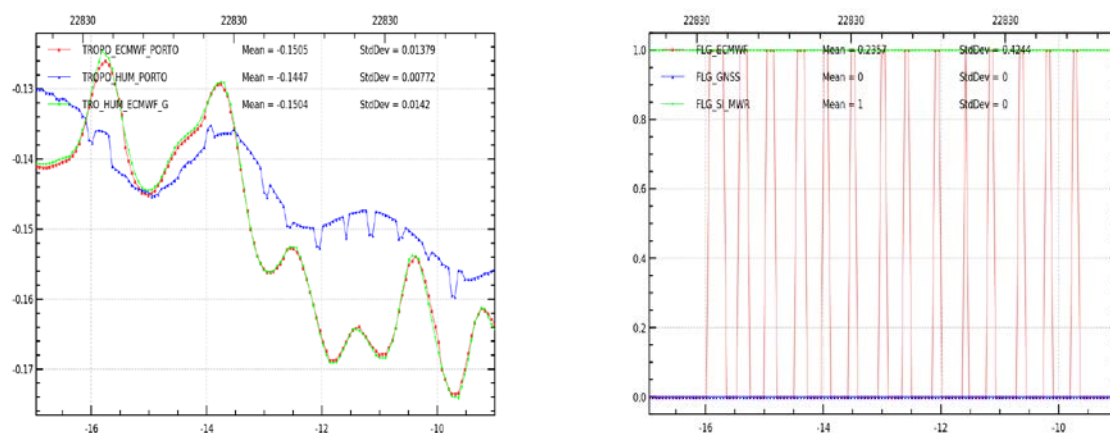


Figure 14: (Left panel) ECMWF WTC from U. Porto dataset (red), ECMWF WTC updated at CLS (green) and the DComb WTC (blue) along the track 82 cycle 32 as function of the latitude. (Right panel). The associated flags for ECMWF, GNSS and SI_MWR.

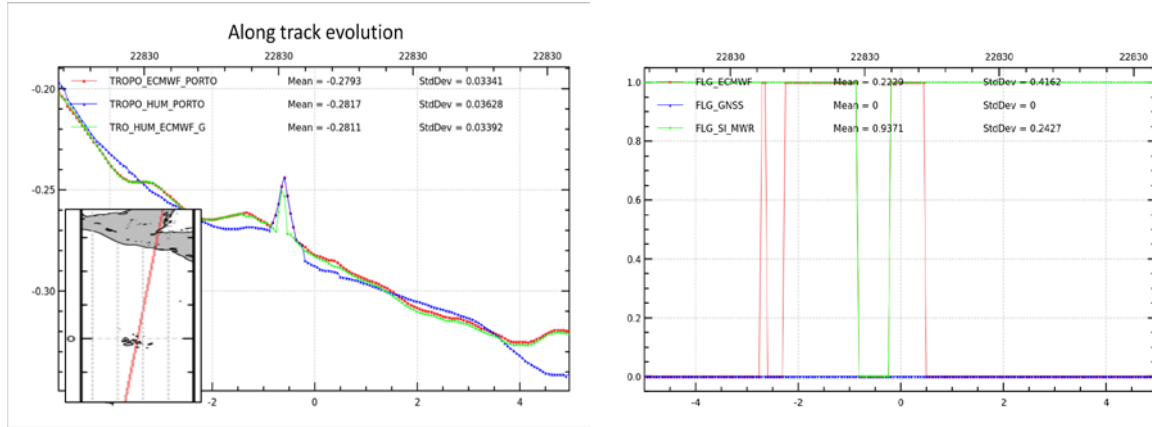


Figure 15: (Left panel) ECMWF WTC from U. Porto dataset (red), ECMWF WTC updated at CLS (green) and the DComb WTC (blue) along the track 82 cycle 32 as function of the latitude. (Right panel). The associated flags for ECMWF, GNSS and SI_MWR.

The Figure 14 and Figure 15 also highlight slight discrepancies between the ECMWF WTC used in the computation of the DComb WTC (at the point location for which the number of observations is lower than 4) and the most recent ECMWF WTC (run on Gaussian global grid). These differences are represented globally in Figure 16 for July 2012 and January 2013. We notice slight differences as high as 1cm which vary geographically and over time. It is difficult to evaluate their impact on the calculation of the DComb WTC by OA.

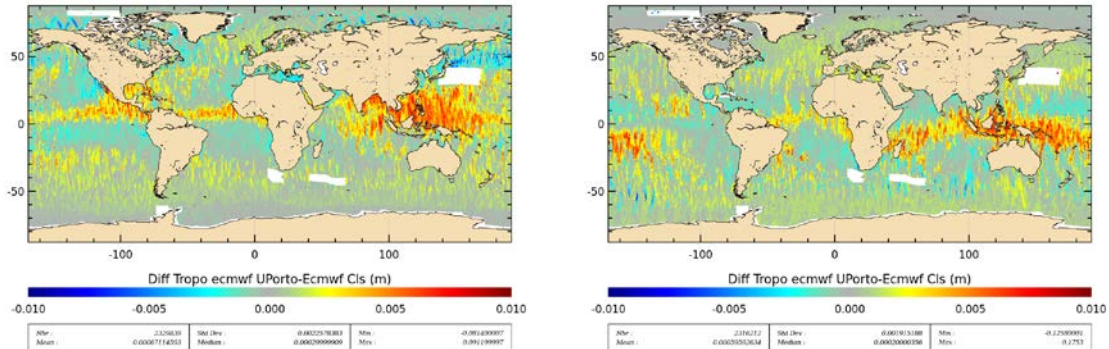


Figure 16: Map of the differences of the WTC computed with the ECMWF model from U. Porto and with the Gaussian ECMWF grid model in July 2012 (left panel) and January 2013 (right panel).

4. Conclusion

The assessment of the DComb WTC has been performed in global (except in SARin mode areas), covering all oceanic waters in the scope of the CP40 project: Open Ocean, Polar Ocean and Coastal Ocean. This improved solution is of particular interest for altimetry missions with no-embarked microwave radiometer, that are affected by the lack of measurements of the water vapour path delay causing a delay in the radar signal which is difficult to correct.

Only 2 months have been used for this assessment. This small time serie prevents from assessing carefully this correction and the conclusions derived from only two months should be confirmed on a longer time series.



Results of this study show that this new correction improves the Cryosat-2 sea surface height accuracy between 50N and 50 S, where we observe a variance reduction at crossovers locally up to 4 cm² and a mean reduction of about 1 cm² over the data set, in comparison to the correction based on the ECMWF meteorological operational model. The DComb correction appears to degrade the performance at higher latitudes (through along-track SLA gain of variance diagnosis). This degradation needs to be confirmed over a longer time series (a full year of data).

Note that the improvement of this correction is achieved notably where the sensor observations are available, while the quality of the DComb WTC is slightly degraded where the ECMWF model is applied. The quality of this method depends on the capacity to collect sensor measurements, although we noticed a quite similar improvement between July 2012 and January 2013.

The DComb correction also improves the performance near the coast, by reducing the SLA variance by 2.4 cm² for distance less than 100 km.

It is important to note that the quality of the DComb WTC could be enhanced with better handling of the along track discontinuities.

5. References

[Fernandes et al., 2010]: Fernandes et al, IEEE Geosc. And Rem Sens Letters, Vol 7, no 3, July 2010.